Journal of Biomedical Optics

SPIEDigitalLibrary.org/jbo

# Infrared spectroscopic analysis of human and bovine articular cartilage proteoglycans using carbohydrate peak or its second derivative

Lassi Rieppo
Tommi Närhi
Heikki J. Helminen
Jukka S. Jurvelin
Simo Saarakkala
Jarno Rieppo

SPIE

TECHNICAL NOTE

# Infrared spectroscopic analysis of human and bovine articular cartilage proteoglycans using carbohydrate peak or its second derivative

**Lassi Rieppo,[a,b] Tommi Närhi,[c] Heikki J. Helminen,[c] Jukka S. Jurvelin,[a] Simo Saarakkala,[d,e] and Jarno Rieppo[c,f]**
[a]University of Eastern Finland, Department of Applied Physics, FI-70211 Kuopio, Finland
[b]Kuopio University Hospital, Department of Clinical Neurophysiology, FI-70029 Kuopio, Finland
[c]University of Eastern Finland, Institute of Biomedicine, FI-70211 Kuopio, Finland
[d]University of Oulu, Institute of Biomedicine, Department of Medical Technology, FI-90014 Oulu, Finland
[e]Oulu University Hospital, Department of Diagnostic Radiology, FI-90029 Oulu, Finland
[f]Iisalmi Hospital, FI-74101 Iisalmi, Finland

**Abstract.** Fourier transform infrared (FTIR) microspectroscopy has been used to estimate the spatial proteoglycan (PG) and collagen contents in articular cartilage (AC). However, it is not clear whether the results of FTIR analyses are consistent between different species. Our aim was to clarify how three different FTIR PG parameters in use, i.e., the integrated absorbance in the carbohydrate region, the carbohydrate/amide I ratio, and the second derivative peak at 1062 $cm^{-1}$, can indicate the densitometrically assessed (reference method) spatial PG content in a sample set consisting of osteoarthritic human and bovine AC samples. The results show that all the parameters can accurately reflect the PG content, when the species are analyzed separately. When all samples are pooled, the correlation with the reference method is high ($r = 0.760$, $n = 104$) for the second derivative peak at 1062 $cm^{-1}$ and is significantly lower ($p < 0.05$) for the carbohydrate region ($r = 0.587$, $n = 104$) and for the carbohydrate/amide I ratio ($r = 0.579$, $n = 104$). Therefore, the analysis of the carbohydrate region may provide inconsistent results, if the cartilage samples from different species are in use. Based on the present study, second derivative analysis yields more consistent results for human and bovine cartilages.  [DOI: 10.1117/1.JBO.18.9.097006]

Keywords: cartilage; proteoglycans; Fourier transform infrared spectroscopy; derivative spectroscopy; imaging.

Paper 130465TNR received Jul. 3, 2013; revised manuscript received Aug. 19, 2013; accepted for publication Aug. 29, 2013; published online Sep. 24, 2013.

## 1 Introduction

Articular cartilage (AC) is a specialized form of hyaline cartilage that covers the ends of long bones in synovial joints. AC bears the load that is directed to bones during joint motion. Together with synovial fluid, AC makes the motion between articulating bones nearly frictionless. Unique properties of AC are due to its structural components, which are inhomogeneously distributed throughout the tissue depth.[1] About 70% to 80% of total weight of AC is water, and more than 95% of AC dry matter consists of collagen and proteoglycans (PGs).[2,3]

Osteoarthritis (OA) is the most common degenerative joint disease in the world. OA induces dramatic changes in the composition of AC, which impairs normal joint function.[4] Sensitive imaging methods are needed to characterize the disease progression. In Fourier transform infrared (FTIR) microspectroscopy, biochemical composition of the tissue is analyzed by its infrared absorption properties. The main advantage of the method is its ability to produce biochemical images from unstained histological sections. Provided that the required specificity for different tissue components is reached, detailed characterization of AC composition could be established with a micron-level spatial resolution.

FTIR microspectroscopic analyses of collagen and PG contents in AC are mainly carried out by calculating integrated peak areas.[5,6] Specificity of the currently used univariate method for PGs, the integrated absorbance of the carbohydrate region, has been questioned.[7–9] This arises from the extensive overlap between the collagen and the PG absorption peaks, as seen from the pure compound spectra.[5] Curve fitting and second derivative spectroscopy have been suggested to reduce the spectral overlap between collagen and PGs.[9,10] Second derivative spectroscopy is more appealing of these two, as it is a mathematically objective procedure and requires no optimization of parameters. We have recently evaluated the contribution of collagen and PGs to the second derivative peaks of AC FTIR spectra by enzymatic removal of PGs.[10] In the experiment, two PG second derivative peaks that had little or no overlap with collagen were found.

It is known that the amount of collagen and PGs varies among sites within cartilage, with age, with OA progression, and between species.[11–14] Furthermore, since the FTIR spectra of collagen and PGs overlap, it would be important that a FTIR-derived compositional parameter is independent of other major macromolecular components in AC. Our aim in this study was to clarify how the traditional FTIR PG parameter, i.e., the integrated absorbance in the carbohydrate region (with or without normalization with amide I absorbance) and recently introduced

Address all correspondence to: Lassi Rieppo, University of Eastern Finland, Department of Applied Physics, POB 1627, 70211 Kuopio, Finland. Tel: +358-50-3759310; Fax: +358-17-163032; E-mail: lassi.rieppo@uef.fi

0091-3286/2013/$25.00 © 2013 SPIE

FTIR PG parameter, the second derivative peak at 1062 $cm^{-1}$, perform in the analysis of the PG content independent of the species. To answer this aim, we reanalyzed and combined the data from our earlier studies consisting of both human and bovine AC samples.[15–17] We hypothesized that the second derivative-based parameter would be less dependent on the species investigated than the carbohydrate region.

## 2 Materials and Methods

### 2.1 *Bovine Articular Cartilage Samples*

The samples were originally collected and prepared in an earlier study.[16] The sample set consisted of healthy and osteoarthritic bovine patellae ($n = 32$). Cylindrical osteochondral samples ($d = 19$ mm) were prepared. A piece of each sample was fixed with 10% formalin and dehydrated and embedded in paraffin.

### 2.2 *Human Articular Cartilage Samples*

Human samples were originally collected and prepared in an earlier study.[15] Osteochondral samples ($n = 72$) were prepared from the patellae of the right knees of 14 cadaveric human donors (age 55 ± 18 years). Six samples ($d = 4$ mm) from different locations (superomedial, superolateral, central medial, central lateral, inferomedial, and inferolateral) were prepared from each patella. Subsequently, the samples were fixed with 10% formalin and dehydrated and embedded in paraffin.

### 2.3 *Histological Grading*

The Osteoarthritis Research Society International (OARSI) histopathology grading system[18] was used to assess OA progression in human AC samples. The samples were divided into three groups: normal ($n = 35$, OARSI grade = 0), early OA ($n = 15$, OARSI grade = 1.0 to 1.5), and advanced OA ($n = 22$, OARSI grade = 3.0 to 4.5).[7,15,19] Bovine samples were not divided into subgroups.

### 2.4 *FTIR Microspectroscopic Measurements*

FTIR microspectroscopic data originate from our earlier studies.[7,15,17] FTIR microspectroscopic measurements were carried out using a Perkin Elmer Spotlight 300 FT-IR imaging system (Perkin Elmer, Shelton, Connecticut). Five-micrometer-thick dewaxed sections were placed onto the 2-mm-thick ZnSe windows and measured in transmission mode using spectral resolution of 4 $cm^{-1}$. Human AC samples were measured using 6.25-$\mu$m pixel size, whereas 25-$\mu$m pixel size was used for bovine AC samples. All spectral preprocessing and data analysis were carried out using Matlab software (R2010a, The MathWorks, Inc., Natick, Massachusetts). The spectra of each measurement were first averaged over the measured width to obtain a single spectrum for each depth. The second derivative spectra were calculated using the Savitzky–Golay algorithm with seven smoothing points.[20] PG content was estimated by calculating the following parameters: the integrated absorbance of the carbohydrate region (984 to 1140 $cm^{-1}$), the ratio of the carbohydrate region to amide I region (1584 to 1720 $cm^{-1}$) [Fig. 1(a)], and the absolute value of the second derivative peak located at 1062 $cm^{-1}$ [Fig. 1(b)]. The obtained depth-wise profiles were resampled to 100 points.

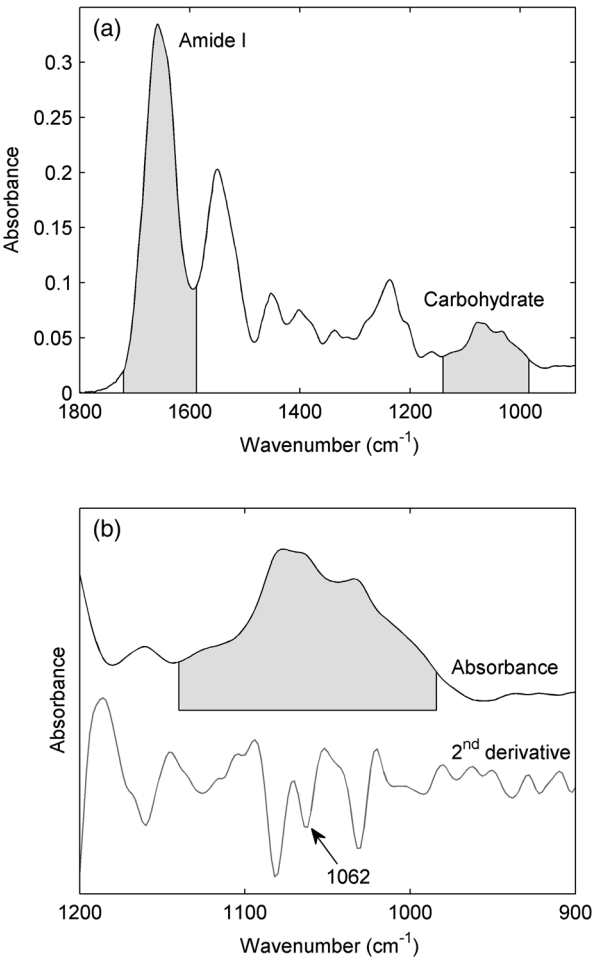


**Fig. 1** (a) Fourier transform infrared (FTIR) spectrum of human articular cartilage (AC). Amide I (1584 to 1720 $cm^{-1}$) and the carbohydrate region (984 to 1140 $cm^{-1}$) are marked by gray shading. (b) FTIR spectrum of human AC at the carbohydrate region (black line) and its second derivative (gray line). The part of the spectrum that is traditionally used for the proteoglycan (PG) analysis is marked by gray shading (984 to 1140 $cm^{-1}$). The second derivative peak at 1062 $cm^{-1}$ that is also used for the PG analysis is indicated by an arrow.

### 2.5 *Digital Densitometry*

Optical density (OD) of Safranin O-stained sections was measured using semiquantitative digital densitometry (DD) to serve as a reference for PG distribution of the samples.[21,22] Three-micrometer-thick sections were prepared and dewaxed before staining. Safranin O binds stoichiometrically to negatively charged glycosaminoglycans of PGs. Therefore, the staining intensity is linearly related to the amount of PGs in AC. Setup is built upon Leitz-Ortholux light microscope (Leitz, Wetzlar, Germany) equipped with 4× Fluotar-objective (Leitz) and a monochromator ($\lambda = 492$ nm, ±1%, Optometrics Inc., Ayer, Massachusetts). 12-bit grayscale images were digitized using Photometrics CH250/A Peltier element-cooled CCD-camera (Photometrics Inc., Tucson, Arizona). Instrumentation was calibrated using a set of neutral density filters from 0 to 3.3 absorbance units (Schott AG, Mainz, Germany). The absorbance is linear under the aforementioned absorbance area. The data of each sample were averaged to obtain a depth-wise PG profile. Subsequently, the profiles were resampled to 100 points.

### 2.6 *Determination of the Histological Zones of AC*

Polarized light microscopy was used to determine the superficial, middle, and deep zones in each OA group of human AC samples. An enhanced polarized light microscopy system built upon Leitz Ortholux II POL (Leitz) was used for this purpose.[23] Details of the determination of the histological zones can be found from an earlier study.[24] For bovine samples, the first 75 $\mu$m of the AC surface was regarded as the superficial layer.[25]

### 2.7 *Data Analysis*

Pearson's linear correlation analysis was used to compare the FTIR PG contents with the reference (OD) information. The correlation analysis was conducted for bulk values and for mean values in different histological zones. The significance of the difference between the correlation coefficients was tested using a statistical test of dependent correlations described by Steiger.[26] The limit of statistical significance was set to $p < 0.05$.

## 3 Results

Linear correlations between the integrated absorbance in the carbohydrate region and OD were high ($r > 0.6$) in all human sample groups and histological zones except in the superficial zone ($r = 0.297$, $n = 72$). Similar results were seen in the bovine samples: the correlation with bulk values was $r = 0.708$, but the correlation in the superficial zone was weak ($r = 0.267$, $n = 32$). In general, values of the integrated absorbance in the carbohydrate region were lower in human samples than in bovine samples, even though the OD values were quite similar. When human and bovine samples were pooled together [Fig. 2(a)], the bulk correlation with OD was weaker ($r = 0.587$, $n = 104$) than when the groups were analyzed separately ($r = 0.838$, $n = 72$ and $r = 0.708$, $n = 32$ in human and bovine samples, respectively).

The results of the carbohydrate/amide I ratio were similar to those of the carbohydrate region alone. Most notable differences between these two parameters were seen in the advanced OA group of human samples, as the ratio parameter did not correlate significantly with OD in any of the analyzed layers (Table 1). The bulk correlations with OD values were significant in both human ($r = 0.648$, $n = 72$) and bovine ($r = 0.696$, $n = 32$) samples. When the samples were pooled together, the correlation with OD values was weaker ($r = 0.579$, $n = 104$) [Fig. 2(b)].

Linear correlation coefficients between the intensity of the second derivative peak at 1062 cm$^{-1}$ with OD values were similar to those between the carbohydrate region and OD in both sample groups (Table 1). The peak at 1062 cm$^{-1}$ correlated better with OD in the superficial zone of human samples ($r = 0.500$) than the carbohydrate region did ($r = 0.297$), but

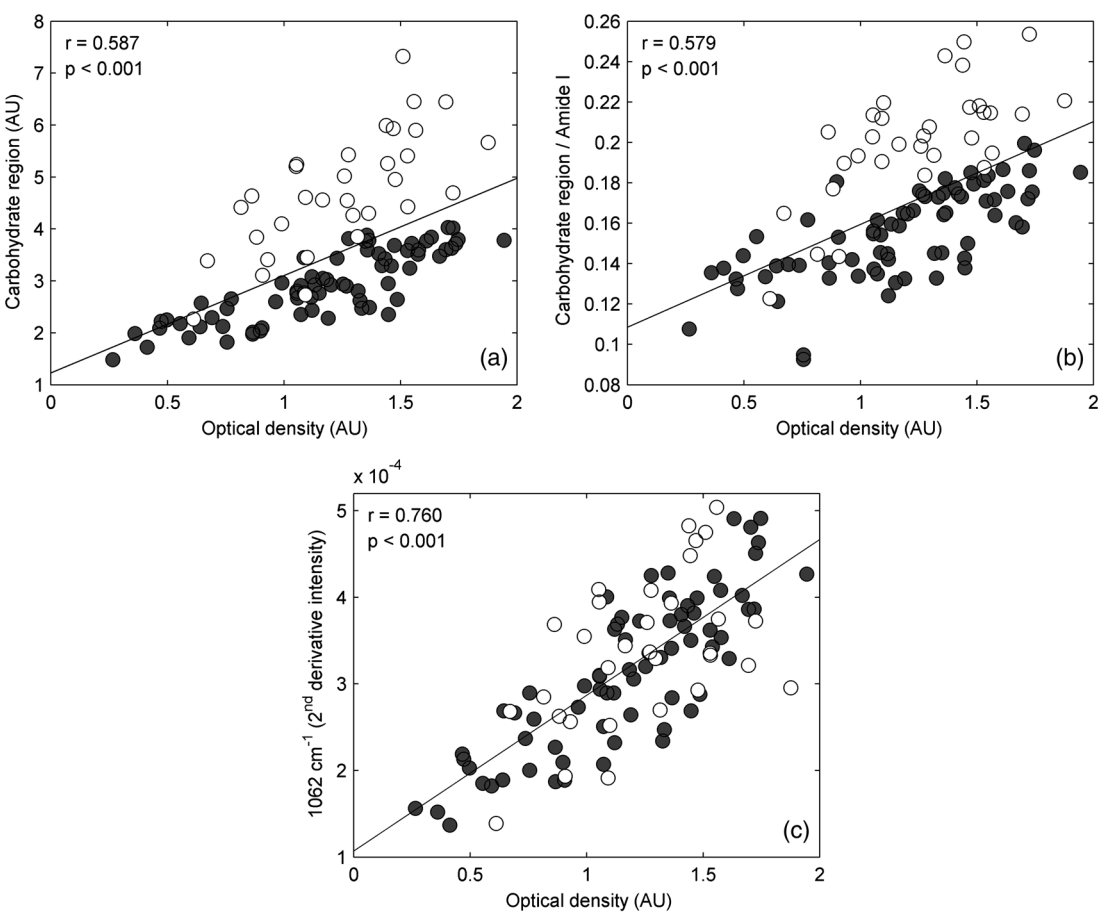


**Fig. 2** Scatter plots between the optical density (OD) of Safranin O (reference estimate for PG content) and different FTIR PG parameters: (a) the integrated absorbance in the carbohydrate region (984 to 1140 cm$^{-1}$), (b) the ratio of the integrated absorbance in the carbohydrate region to that of the amide I (1584 to 1720 cm$^{-1}$), and (c) the intensity of the second derivative peak at 1062 cm$^{-1}$. The human and bovine samples are marked with gray and white circles, respectively.

**Table 1** Linear correlation coefficients between the Fourier transform infrared (FTIR) proteoglycan (PG) parameters and the optical density (OD) of Safranin O (reference estimate for PG content). The correlation coefficients are statistically significant unless otherwise indicated.

| Group | Zone | Carbohydrate | Carbohydrate/Amide I | 1062 $cm^{-1}$ |
|---|---|---|---|---|
| Human samples ($n = 72$) | | | | |
| Normal ($n = 35$) | Bulk | 0.709 | 0.700 | 0.697 |
| | Superficial | 0.448 | 0.655[a] | 0.514 |
| | Middle | 0.721 | 0.820 | 0.728 |
| | Deep | 0.706 | 0.620 | 0.683 |
| Early osteoarthritis (OA) ($n = 15$) | Bulk | 0.864 | 0.747 | 0.779 |
| | Superficial | 0.241 (N.S.) | 0.192 (N.S.) | 0.172 (N.S.) |
| | Middle | 0.822 | 0.805 | 0.732 |
| | Deep | 0.639 | 0.720 | 0.764 |
| Advanced OA ($n = 22$) | Bulk | 0.762[b] | 0.318 (N.S.) | 0.824[b] |
| | Superficial | 0.131 (N.S.) | 0.119 (N.S.) | 0.358 (N.S.) |
| | Middle | 0.615[b] | 0.203 (N.S.) | 0.733[b] |
| | Deep | 0.764[b] | 0.366 (N.S.) | 0.828[b] |
| All | Bulk | 0.838[b] | 0.648 | 0.833[b] |
| | Superficial | 0.297 | 0.312 | 0.500 |
| | Middle | 0.804[b] | 0.700 | 0.832[b] |
| | Deep | 0.828[b] | 0.671 | 0.828[b] |
| Bovine samples ($n = 32$) | Bulk | 0.708[c] | 0.696 | 0.516 |
| | Superficial | 0.267 (N.S.) | 0.349 | 0.262 (N.S.) |
| All samples ($n = 104$) | Bulk | 0.587 | 0.579 | 0.760[a,b] |

N.S. = Not significant.
[a]Significantly higher $r$ compared with that of the carbohydrate peak ($p < 0.05$).
[b]Significantly higher $r$ compared with that of the carbohydrate/amide I peak ($p < 0.05$).
[c]Significantly higher $r$ compared with that of the second derivative peak at 1062 $cm^{-1}$ ($p < 0.05$).

the difference between the correlation coefficients was not statistically significant ($p = 0.15$). The intensities of the second derivative peak at 1062 $cm^{-1}$ were similar in both sample groups. Consequently, the bulk correlation was $r = 0.760$ ($n = 104$) when human and bovine samples were pooled together [Fig. 2(c)]. Linear correlations between the FTIR-based parameters and OD of Safranin O have been listed in Table 1.

## 4 Discussion

The aim in this study was to evaluate how the integrated absorbance in the carbohydrate region, the carbohydrate/amide I ratio, and the intensity of the second derivative peak at 1062 $cm^{-1}$ perform in the FTIR analysis of the spatial PG content in AC independent of the species. The results show that all parameters perform well when the species are analyzed separately. However, when human and bovine samples are pooled together, these FTIR parameters perform inconsistently. The linear correlation with the reference method is good in the case of second derivative peak at 1062 $cm^{-1}$, but not in the case of the carbohydrate region-based parameters. In general, the values of the carbohydrate parameters seem to be higher in bovine samples than in human samples. In addition to PG vibrations, the carbohydrate region also contains collagen vibrations.[5,8] The difference in the carbohydrate region values between the species is most likely explained by the differences in the total collagen content between the cartilages of these two species. In principle, the carbohydrate/amide I ratio parameter takes into account the variable collagen content, as amide I is used as an estimate for the collagen content. However, also the values of the ratio were higher in bovine samples than in human samples. The second derivative peak analyzed in this study is a small part of the carbohydrate region. It has been assigned to C O vibrations of carbohydrates and $SO_3^-$ vibrations of sulfates found in glycosaminoglycans.[27,28] The values of this second derivative

peak were similar in both the species. This suggests that the second derivative peak contains significantly less contribution from the collagen vibrations than the whole carbohydrate region.

All the parameters reflected closely the bulk PG content as well as the PG content in the middle and deep layers of AC. However, they showed weaker correlations in the superficial zone. The correlation of second derivative peak at 1062 $cm^{-1}$ was little higher than those of the carbohydrate region or the carbohydrate/amide I ratio in the superficial zone in human AC, although the differences were not statistically significant. The superficial zone is the thinnest histological zone in AC. In our FTIR measurements, the superficial zone comprises only a few pixels depending on the pixel size in use. Weak correlations might be partially explained by the fact that it is difficult to accurately match thin zones between the FTIR and DD measurements. This might be a significant problem especially in case of OA samples, as the degenerated cartilage surface is irregular. Nevertheless, it is evident that the univariate FTIR PG parameters can be inaccurate when assessing the PGs in the superficial zone of AC.[7,9]

OA induces changes in the biochemical composition of AC. One of the first signs of OA is the loss of the PGs.[4] In this study, it was shown that FTIR spectroscopy accurately detects the differences in the PG content in healthy and osteoarthritic human and bovine ACs. Second derivative analysis reduces the overlap between the collagen and the PG absorption peaks. It is possible to compare the PG content between the species only if the parameter is independent of other macromolecules. This study suggests that the second derivative peak at 1062 $cm^{-1}$ is independent of the collagen content and enables direct comparison of the parameter values between different species.

Univariate analysis is applicable when nonoverlapping peaks are found either directly or after preprocessing, e.g., after differentiation (derivative spectra). Multivariate models, such as principal component regression and partial least squares regression, are also suitable for overlapping spectra. Recently, multivariate models have been used to predict the AC composition in several independent studies.[8,29–31] These studies have shown that multivariate models are superior to univariate parameters when AC composition is analyzed.[8,29,30] Another advantage of multivariate models is that they provide an estimation of actual concentration values, as they are calibrated against a reference method. Therefore, multivariate models enable real-quantitative analysis. However, if a calibrated multivariate model is not available for use, second derivative spectroscopy offers a feasible and improved analysis of PGs over that of the traditional methods.

## Acknowledgments

The study was funded by the North Savo fund of the Finnish Cultural Foundation, strategic funding of the University of Eastern Finland, strategic funding of the University of Oulu (Project 24001200), and Kuopio University Hospital (EVO Grant 5041724). Atria Oyj is acknowledged for supplying the bovine sample material. We thank Professor Ilkka Kiviranta, MD, PhD; Panu Kiviranta, MD, PhD; and Eveliina Lammentausta, PhD for the original human sample material. Mrs. Eija Rahunen and Mr. Kari Kotikumpu are acknowledged for their skilful technical assistance with tissue and sample preparations.

## References

1. J. Dunham et al., "A reappraisal of the structure of normal canine articular cartilage," *J. Anat.* **157**, 89–99 (1988).
2. J. A. Buckwalter and H. J. Mankin, "Articular cartilage: tissue design and chondrocyte-matrix interactions," *Instr. Course Lect.* **47**, 477–486 (1998).
3. C. A. McDevitt, "Biochemistry of articular cartilage. Nature of proteoglycans and collagen of articular cartilage and their role in ageing and in osteoarthrosis," *Ann. Rheum. Dis.* **32**(4), 364–378 (1973).
4. J. A. Buckwalter and H. J. Mankin, "Articular cartilage: degeneration and osteoarthritis, repair, regeneration, and transplantation," *Instr. Course Lect.* **47**, 487–504 (1998).
5. N. P. Camacho et al., "FTIR microscopic imaging of collagen and proteoglycan in bovine cartilage," *Biopolymers* **62**(1), 1–8 (2001).
6. P. A. West et al., "Fourier transform infrared imaging spectroscopy analysis of collagenase-induced cartilage degradation," *J. Biomed. Opt.* **10**(1), 014015–014015-6 (2005).
7. S. Saarakkala and P. Julkunen, "Specificity of Fourier transform infrared (FTIR) microspectroscopy to estimate depth-wise proteoglycan content in normal and osteoarthritic human articular cartilage," *Cartilage* **1**(4), 262–269 (2010).
8. J. Yin and Y. Xia, "Macromolecular concentrations in bovine nasal cartilage by Fourier transform infrared imaging and principal component regression," *Appl. Spectrosc.* **64**(11), 1199–1208 (2010).
9. L. Rieppo et al., "Quantitative analysis of spatial proteoglycan content in articular cartilage with Fourier transform infrared imaging spectroscopy: critical evaluation of analysis methods and specificity of the parameters," *Microsc. Res. Tech.* **73**(5), 503–512 (2010).
10. L. Rieppo et al., "Application of second derivative spectroscopy for increasing molecular specificity of Fourier transform infrared spectroscopic imaging of articular cartilage," *Osteoarthr. Cartilage* **20**(5), 451–459 (2012).
11. J. A. Buckwalter and H. J. Mankin, "Instructional course lectures, the American Academy of Orthopaedic Surgeons—articular cartilage. Part I: tissue design and chondrocyte-matrix interactions*†," *J. Bone Joint Surg.* **79**(4), 600–611 (1997).
12. M. M. Temple et al., "Age- and site-associated biomechanical weakening of human articular cartilage of the femoral condyle," *Osteoarthr. Cartilage* **15**(9), 1042–1052 (2007).
13. A. K. Williamson et al., "Tensile mechanical properties of bovine articular cartilage: variations with growth and relationships to collagen network components," *J. Orthop. Res.* **21**(5), 872–880 (2003).
14. A. K. Williamson, A. C. Chen, and R. L. Sah, "Compressive properties and function-composition relationships of developing bovine articular cartilage," *J. Orthop. Res.* **19**(6), 1113–1121 (2001).
15. P. Kiviranta et al., "Indentation diagnostics of cartilage degeneration," *Osteoarthr. Cartilage* **16**(7), 796–804 (2008).
16. S. Saarakkala et al., "Ultrasound indentation of normal and spontaneously degenerated bovine articular cartilage," *Osteoarthr. Cartilage* **11**(9), 697–705 (2003).
17. L. Rieppo et al., "Prediction of compressive stiffness of articular cartilage using Fourier transform infrared spectroscopy," *J. Biomech.* **46**(7), 1269–1275 (2013).
18. K. P. Pritzker et al., "Osteoarthritis cartilage histopathology: grading and staging," *Osteoarthr. Cartilage* **14**(1), 13–29 (2006).
19. S. Saarakkala et al., "Depth-wise progression of osteoarthritis in human articular cartilage: investigation of composition, structure and biomechanics," *Osteoarthr. Cartilage* **18**(1), 73–81 (2010).
20. A. Savitzky and M. J. E. Golay, "Smoothing and differentiation of data by simplified least squares procedures," *Anal. Chem.* **36**(8), 1627–1639 (1964).
21. I. Kiviranta et al., "Microspectrophotometric quantitation of glycosaminoglycans in articular cartilage sections stained with Safranin O," *Histochemistry* **82**(3), 249–255 (1985).
22. K. Kiraly et al., "Application of selected cationic dyes for the semiquantitative estimation of glycosaminoglycans in histological sections of articular cartilage by microspectrophotometry," *Histochem. J.* **28**(8), 577–590 (1996).
23. J. Rieppo et al., "Practical considerations in the use of polarized light microscopy in the analysis of the collagen network in articular cartilage," *Microsc. Res. Tech.* **71**(4), 279–287 (2008).

24. P. Julkunen et al., "Characterization of articular cartilage by combining microscopic analysis with a fibril-reinforced finite-element model," *J. Biomech.* **40**(8), 1862–1870 (2007).
25. M. J. Nissi et al., "Proteoglycan and collagen sensitive MRI evaluation of normal and degenerated articular cartilage," *J. Orthop. Res.* **22**(3), 557–564 (2004).
26. J. H. Steiger, "Tests for comparing elements of a correlation matrix," *Psychol. Bull.* **87**(2), 245–251 (1980).
27. R. Servaty et al., "Hydration of polymeric components of cartilage—an infrared spectroscopic study on hyaluronic acid and chondroitin sulfate," *Int. J. Biol. Macromol.* **28**(2), 121–127 (2001).
28. A. Kohler et al., "Multivariate image analysis of a set of FTIR microspectroscopy images of aged bovine muscle tissue combining image and design information," *Anal. Bioanal. Chem.* **389**(4), 1143–1153 (2007).
29. J. Yin, Y. Xia, and M. Lu, "Concentration profiles of collagen and proteoglycan in articular cartilage by Fourier transform infrared imaging and principal component regression," *Spectrochim. Acta A Mol. Biomol. Spectrosc.* **88**, 90–96 (2012).
30. L. Rieppo et al., "Fourier transform infrared spectroscopic imaging and multivariate regression for prediction of proteoglycan content of articular cartilage," *PLoS One.* **7**(2), e32344 (2012).
31. A. Hanifi et al., "Fourier transform infrared imaging and infrared fiber optic probe spectroscopy identify collagen type in connective tissues," *PLoS ONE.* **8**(5), e64822 (2013).